

Article

Rheological Investigation of Highly Filled Copper(II) Oxide Nanosuspensions to Optimize Precursor Particle Content in Reductive Laser-Sintering

Kay Bischoff ^{1,*} , Dominik Mücke ¹ , Andreas Schubert ², Cemal Esen ³  and Ralf Hellmann ¹ 

¹ Applied Laser and Photonics Group, University of Applied Sciences Aschaffenburg, Würzburger Straße 45, 63743 Aschaffenburg, Germany; dominik.muecke@th-ab.de (D.M.); ralf.hellmann@th-ab.de (R.H.)

² Anton Paar Germany GmbH, Hellmuth-Hirth-Strasse 6, 73760 Ostfildern-Scharnhausen, Germany; andreas.schubert@anton-paar.com

³ Applied Laser Technologies, Ruhr University Bochum, Universitätsstraße 150, 44801 Bochum, Germany; esen@lat.rub.de

* Correspondence: kay.bischoff@th-ab.de

Abstract: In this article, the particle concentration of finely dispersed copper(II) oxide nanosuspensions as precursors for reductive laser sintering (RLS) is optimized on the basis of rheological investigations. For this metallization process, a smooth, homogeneous and defect-free precursor layer is a prerequisite for adherent and reproducible copper structures. The knowledge of the rheological properties of an ink is crucial for the selection of a suitable coating technology as well as for the adjustment of the ink formulation. Different dilutions of the nanosuspension were examined for their rheological behavior by recording flow curves. A strong shear thinning behavior was found and the viscosity decreases exponentially with increasing dilution. The viscoelastic behavior was investigated by a simulated doctor blade coating process using three-interval thixotropy tests. An overshoot in viscosity is observed, which decreases with increasing thinning of the precursor. As a comparison to these results, doctor blade coating of planar glass and polymer substrates was performed to prepare precursor layers for reductive laser sintering. Surface morphology measurements of the resulting coatings using laser scanning microscopy and rheological tests show that homogeneous precursor layers with constant thickness can be produced at a particle–solvent ratio of 1.33. A too-high particle content results in an irregular coating layer with deep grooves and a peak-to-valley height S_z of up to 7.8 μm . Precise dilution control allows the fabrication of smooth surfaces with a S_z down to 1.5 μm .

Keywords: reductive laser sintering; nanosuspension; rheology; laser digital patterning; CuO



check for updates

Citation: Bischoff, K.; Mücke, D.; Schubert, A.; Esen, C.; Hellmann, R. Rheological Investigation of Highly Filled Copper(II) Oxide Nanosuspensions to Optimize Precursor Particle Content in Reductive Laser-Sintering. *Liquids* **2024**, *4*, 382–392. <https://doi.org/10.3390/liquids4020019>

Academic Editor: Enrico Bodo

Received: 19 February 2024

Revised: 18 March 2024

Accepted: 3 April 2024

Published: 24 April 2024



Copyright: © 2024 by the authors. Licensee MDPI, Basel, Switzerland. This article is an open access article distributed under the terms and conditions of the Creative Commons Attribution (CC BY) license (<https://creativecommons.org/licenses/by/4.0/>).

1. Introduction

Recently, intensive research has been conducted into technologies that can replace conventional mask- and vacuum-based lithography processes for the production of electronic conductors, sensors and actuators [1–3]. Laser direct writing processes in particular offer enormous flexibility in terms of the layout to be produced and make thermal sintering, in which the substrate to be coated must be fully heated, obsolete. This means that even temperature-sensitive substrates such as polymers can be successfully metallized [4,5]. In addition, the laser, especially with ultrashort laser pulses, is an emerging tool for processing a wide variety of material classes with the highest precision, so that hybrid production processes for applications such as lab-on-chip systems can be realized [6,7].

By substituting noble metals with copper, an enormous increase in cost efficiency can be achieved with comparable performance and conductivity [4]. However, the oxidation tendency of copper has led to a preference for precursor-based processes such as reductive laser sintering [8]. In this technique, stable copper compounds are applied to a substrate under atmospheric process conditions and converted into metallic copper by triggering

a thermochemical reduction and simultaneous sintering. A distinction is made between different types of Cu precursors (PC). In addition to ionic solutions based on copper salts [9–11] or complexes [12] and deep eutectic solvents [13,14], copper oxides in the form of nanoparticles (NPs) suspensions can also be used. This enables a maskless, vacuum-free, flexible and direct writing technology that can be used on a wide range of substrates, such as glass [8,15–17] and polymers [18–20]. A wide range of applications have already been demonstrated. Since the first demonstration of copper(II) oxide NPs as a material for copper PC inks by Kang et al. [8], this form has attracted a great interest in research. Compared to other PC types, this type is favored by high process speeds, compatibility with other laser-based technologies [6,7] and structure resolutions in the range of 10 μm .

The process of reductive laser sintering is divided into several process steps as illustrated in Figure 1. A PC based on copper(II) oxide (CuO) NPs is applied to the substrate surface using a suitable coating process (e.g., spin coating or doctor blade) to form a homogeneous dry layer with a thickness in the micrometer range after drying. The thermochemical reduction of CuO to metallic copper is initiated by selective energy input of the laser beam to metallic Cu particles, which are simultaneously sintered. Finally, the remaining PC can be rinsed off, leaving the resulting conductive structures.

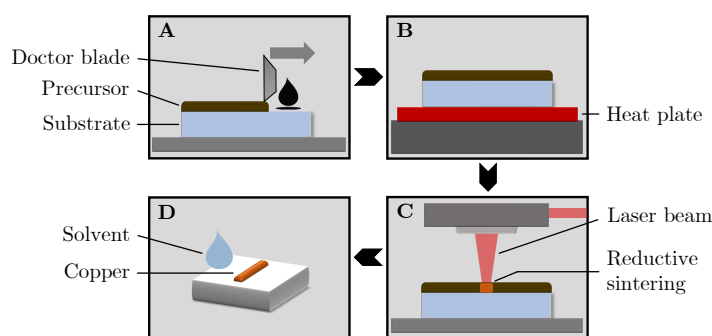


Figure 1. Schematic illustration of reductive laser sintering. (A) coating of PC; (B) drying on a heating plate; (C) selective laser processing of the PC layer; (D) rinsing of the remaining unprocessed PC.

The PCs are essentially based on the solvent ethylene glycol (EG) and the stabilizer polyvinylpyrrolidone (PVP). Arakane et al. [15] already showed that the amount of solvent has a major influence on the resulting PC layer quality and postulated the ideal particle content at 60 wt%, which has been used in a large number of studies by various research groups [6,17,21]. In RLS, a smooth, homogeneous PC layer without defects is the basic prerequisite for adherent and reproducible copper structures. Recently, the production of highly filled, finely dispersed CuO PC for RLS was demonstrated by high-energy ball milling, so that ultra-homogeneous PC layers can be produced without interfering agglomerates. As in other works, the coating composition had to be finely adjusted by adding solvent in order to achieve good coatability [22].

Knowledge of the rheological properties of an ink is crucial for both the selection of a suitable coating technology and for the adjustment of its formulation to achieve homogeneous coating results. In the past, copper(II)-oxide-based nanofluids with water as a solvent have already been investigated in terms of their rheological properties. It was demonstrated that these fluids exhibit shear thinning, pseudoplastic properties and that these characteristics show a strong dependence on concentration [23]. Non-Newtonian properties have also been demonstrated for CuO nanofluids with ethylene glycol as a solvent, as used in reductive laser sintering [24]. However, the investigations here are limited to particle concentrations of up to 1.5 v%, which are not applicable for the coating process. To the best of our knowledge, rheological investigations of highly filled CuO–EG PC in conjunction with coatings for reductive laser sintering have not been performed. Due to the strong influence of particle size and concentration on rheological properties, further investigations are needed to maximize the quality and behavior of such highly filled CuO–PVP–EG precursors.

In this work, the rheological properties of highly filled copper(II) oxide precursor for reductive laser sintering are investigated. The influence of the particle concentration in such a nanosuspension is investigated by recording flow curves and carrying out three-interval thixotropy tests (3ITTs) and validated by coating using a doctor blade process. The target was to adjust the composition of the PC so that homogeneous coating layers can be produced, which form the basis for the production of homogeneous copper structures.

2. Materials and Methods

2.1. Chemicals and Materials

PVP K12 ($2000\text{--}3000\text{ g mol}^{-1}$), EG (>99%) and Ethanol (>99.8%) were purchased from Carl Roth (Karlsruhe, Germany). Powdered CuO NPs (40–80 nm) were obtained from Iolitec (Heilbronn, Germany). Cyclic olefin copolymers (COC) substrates (TOPAS 6017S-04) were purchased from TOPAS Advanced Polymers (Raunheim, Germany). Soda-lime glass slides were sourced from Marienfeld (Lauda-Königshofen, Germany).

2.2. Preparation and Characterization of the Nanosuspension

To prepare the CuO stock suspension, PVP was fully dissolved in EG, and then added to CuO NPs and stirred to a homogeneous paste. The concentrations correspond to the mass ratio CuO:EG = 2.5 and CuO:PVP = 4.62. High-energy ball milling (MM 500 nano, Retsch, Haan, Germany) was utilized to disperse the NPs with a frequency of 35 Hz during a grinding time of 100 min. For efficient milling, ethanol was added to lower the viscosity. Residual ethanol was gently distilled out after dispersion by means of a rotary evaporator (RV 3, IKA). The cooled fluid was degassed by increasing the evacuation.

The particle size distribution of the wet PK was measured in triplicate using a laser diffraction particle size analyzer (SYNC 2B1R DIA, Microtrac, Haan, Germany). Highly diluted PC was dried on a glass slide, to visualize the particles. Images were obtained using an SEM (MAIA3, Tescan, Brno, Czech Republic) at an accelerating voltage of 8 kV in the ultrahigh-resolution mode. The size measurement of the SEM images was performed using the software Gwyddion (Czech Metrology Institute, Jihlava, Czech Republic). For further details on the PC preparation and measurement, we refer readers to our previous publication [22]. After its characterization, the stock PC was diluted stepwise by adding EG. Thus, the mass ratio of CuO NPs and solvent EG (CuO:EG) is gradually decreased from 2.5 to 1.0. Stirring and degassing were performed before further characterization of the new dilution step. The compositions of the nanosuspensions are shown in Table 1.

Table 1. Concentrations and particle–solvent ratios (CuO:EG) of different precursor dilutions.

Suspension No.	CuO:EG Mass Ratio	CuO NP Mass Concentration in wt%	CuO:PVP Mass Ratio
stock	2.50	61.86	
1	2.22	60.00	
2	2.00	58.25	4.62
3	1.67	55.05	
4	1.33	50.85	
5	1.00	45.11	

2.3. Rheological Characterization

The rheological measurements were carried out in triplicate using a Modular Compact Rheometer with a combined motor transducer system (MCR 302e, CMT, Anton Paar, Graz, Austria). A cone–plate setup was used as measuring setup (cf. Figure 2). The cone (CP) had a diameter of 25 mm and an angle of 2° (CP25- 2°). The temperature was controlled by means of Peltier heating of the lower measuring plate (P-PTD220/AIR, Anton Paar, Graz, Austria). All samples were tempered to 23°C for 60 s with a tolerance of $\pm 0.2^\circ\text{C}$ prior to measurement.

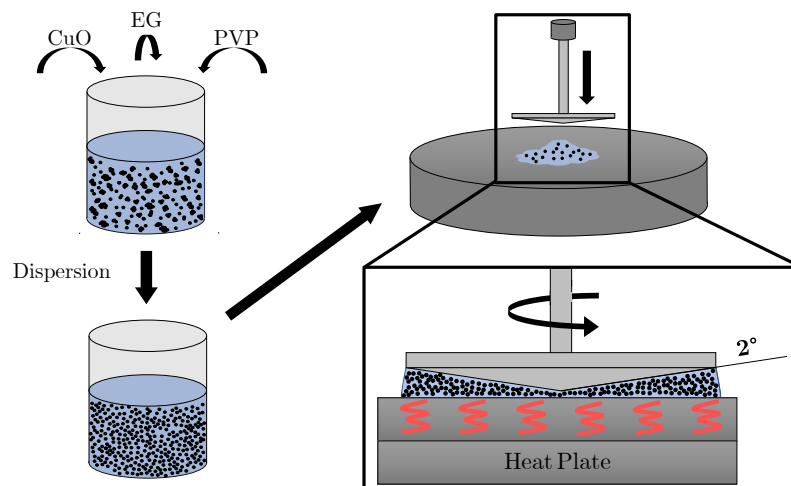


Figure 2. Schematic representation of precursor preparation by high-energy ball milling (left) and rheological measurement of precursors with cone–plate configuration (right).

To measure the PC flow curves, the shear rate $\dot{\gamma}(t)$ was first gradually increased from 0.01 s^{-1} to the maximum value of 1000 s^{-1} and then decreased again. Both measurements were plotted with a logarithmic increase in shear rate. The measured data of the flow curve were also subjected to a logarithmic data point recording, starting from a recording time of 10 s at low shear rates to 1 s at high shear rates. The 3ITT consists of three measurement sections with varying shear rate specifications. Starting with a reference section at 0.5 s^{-1} for 60 s, a loading phase at 400 s^{-1} for 15 s and a structural recovery section at 0.5 s^{-1} for 45 s. A schematic representation of the jump test with the three measurement sections is shown in Figure 3.

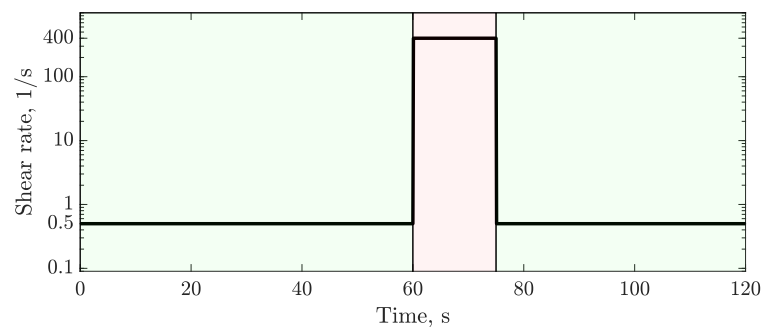


Figure 3. Shear rate profile in the 3ITT to simulate the doctor blade coating process.

2.4. Doctor Blade Coating for Reductive Laser Sintering

The produced CuO PC must be homogeneously coated on the substrate surface to be electrified. To ensure wettability of COC and glass, the substrates were plasma activated (Zepto, Diener, Ebhausen, Germany) for 6 min at 0.2 mbar. The PC was applied to cleaned $50 \times 50 \text{ mm}^2$ COC or $76 \times 52 \text{ mm}^2$ glass substrate and coated using the doctor blade method (ZAA 3000, Proceq, Schwerzenbach, Switzerland). The adjustable applicator was set to a height of $40 \mu\text{m}$ and was moved at a speed of 10 mm s^{-1} . The wet PC was dried at 70°C for 30 min. A comprehensive description of the RLS process is given elsewhere [6,7].

Optical inspection of the PC surface was performed using a digital microscope (DMV6, Leica, Wetzlar, Germany). The surface topography of the dried PC layers was evaluated using a laser scanning microscope (LSM) (VK-X200, Keyence, Osaka, Japan). For this purpose, areas of $6.2 \times 0.5 \text{ mm}^2$ were recorded by stitching 10 partial images with the $20\times$ objective. The characterization of grooves in the coating surface was performed by average surface roughness S_a and peak-to-valley height S_z measurements.

3. Results

3.1. Characterization of the Nanoparticles

To understand the rheological properties of nanosuspensions, it is necessary to know the properties of the particle species, the solvent and other ink components such as the PVP stabilizer and also the particle size and shape [25,26]. The particle size distribution of the nanosuspension was measured using the laser diffraction particle size analyzer, the results being depicted in Figure 4. Two modes are observed at approximately 200 and 500 nm. The percentiles are: $D_{90} = 665 \text{ nm}$, $D_{50} = 290 \text{ nm}$ and $D_{10} = 170 \text{ nm}$, respectively. The suspension is therefore almost free of agglomerates. In addition, the CuO NPs were visualized by SEM and are shown in Figure 4b,c. The nanoplates are measured by SEM to be 100 to 600 nm in size with large aspect ratios and formed loose clusters during the drying process.

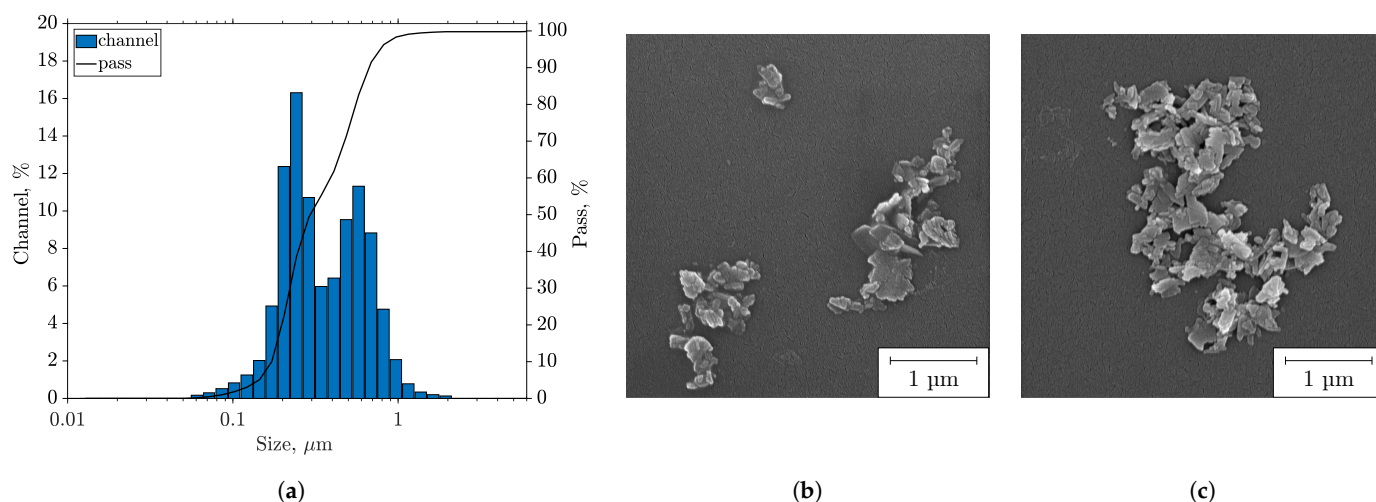


Figure 4. (a) Particle size distribution in the dispersed PC, measured by particle size analyzer. (b,c) dispersed CuO particles inside the RLS PC visualized by SEM.

3.2. Flow Behavior of the Diluted Precursors

The stock solution (EG:CuO 2.5) is too highly filled to be characterizable by rheological tests. Due to the high particle amount, the stock solution behaves more like an elastic solid than a measurable viscoelastic liquid. The size distribution of the particles in the suspension, as well as their shape and charge, are relevant for this. The viscous content is too low; thus, the “paste” does not flow and there is a high probability of wall sliding and, at higher shear rates, gap emptying, which means that there is no rheological basis for a meaningful experiment. For this reason, only the dilution levels 2.22 to 1.0 are shown in Figure 5a in the shear range 0.01 to 1000 s^{-1} . The upward curve in between the shear rate 0.01 to 1 s^{-1} is characterized by a belly. The flow curve only stabilizes from 1 to 1000 s^{-1} . For dispersions 1.00 and 1.67, the flow is more uniform. In Figure 5b, the viscosity evolution for different shear rates ($1, 10, 100, 1000 \text{ s}^{-1}$) is compared with the CuO:EG ratio. The viscosity decreases exponentially with decreasing EG:CuO ratio for all shear rates and is nearly parallel.

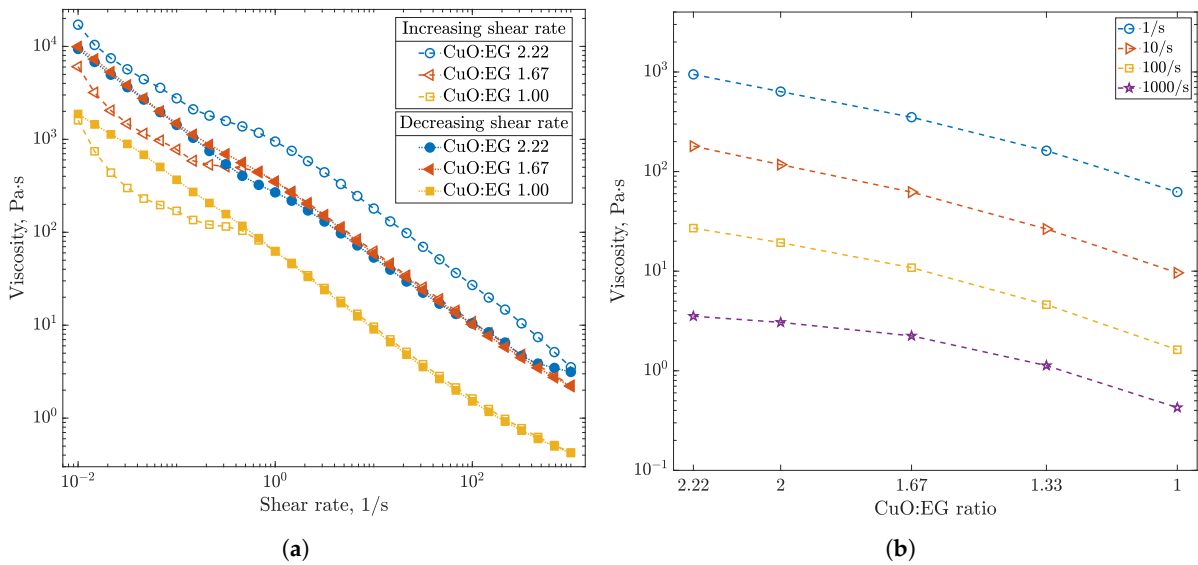


Figure 5. (a) Flow curves of dilutions 2.22, 1.67 and 1.00 measured at increasing (unfilled markers) and decreasing (filled markers) shear rates. (b) Viscosity evolution at different shear rates for increasing dilution of nanosuspensions.

3.3. Viscoelastic Behavior of the Diluted Precursors

The 3ITT represents the application process of the PC to the substrate as given in Figure 6. In the first interval, the sample is loaded under very low shear rates until a uniform laminar flow of the sample is achieved. Initially the viscosity appears to increase but this is due to the sample not being fully laminar (transient viscosity). Application via the doctor blade process is carried out by setting the calculated shear rates in the second section (load) of the doctor blade process. Here, all samples reveal a shear thinning property under the applied shear rate. The two highest filled samples with CuO:EG mass ratios 2.22 and 2.00 also show a further decrease in viscosity over the course of second section. The overshooting of the viscosity values after the loading phase in the third section of the step test is related to inertial effects of the sample as well as its concentration and viscoelastic properties.

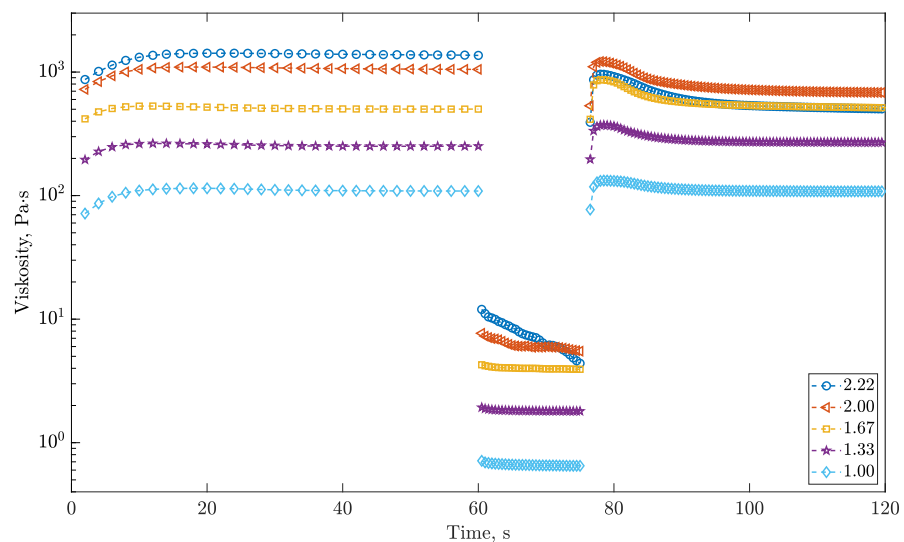


Figure 6. Viscosity as a function of time in the simulation of the doctor blade process using the 3ITT for the various dilutions of the nanosuspensions.

After the overshoot, samples 1.00, 1.33 and 1.67 drop to approximately the viscosity values in interval 1. In contrast, samples 2.00 and 2.22 drop to a lower viscosity. In case of the higher concentrations of 2.00 and 2.22, it cannot be ruled out that coagulates present in the sample were destroyed by the higher shear rate and that the viscosity, therefore, decreased in the subsequent structure formation phase.

3.4. Coating Quality of the Diluted Precursors

All six dilution levels of the PC were coated onto planar COC and glass substrates using doctor blade applicators and then dried. Please note that the following results are reported on COC although the observations were also made on glass as a substrate. The mean surface roughness S_a and peak-to-valley height S_z were measured and are summarized as a function of the particle-to-solvent ratio (CuO:EG) in Figure 7a. For the highest particle concentration in the stock suspension (2.5), a high S_z of about $7.8\ \mu\text{m}$ and S_a of $524\ \text{nm}$ is measured. The surface morphology is also shown at the top of Figure 7b. There appear strongly pronounced grooves in the dry layer. With increasing dilution, the roughness decreases to $S_z = 1.5\ \mu\text{m}$ and $S_a = 197\ \text{nm}$ up to the dilution 1.33 and increases slightly with further dilution. The resulting PC surface of dilution 1.33 is shown at the bottom of Figure 7b. After dilution, the initially observed grooves have almost completely disappeared and there is only a slight waviness in the sub-micrometer range. Please note that these results can also be reproduced when coating glass slides.

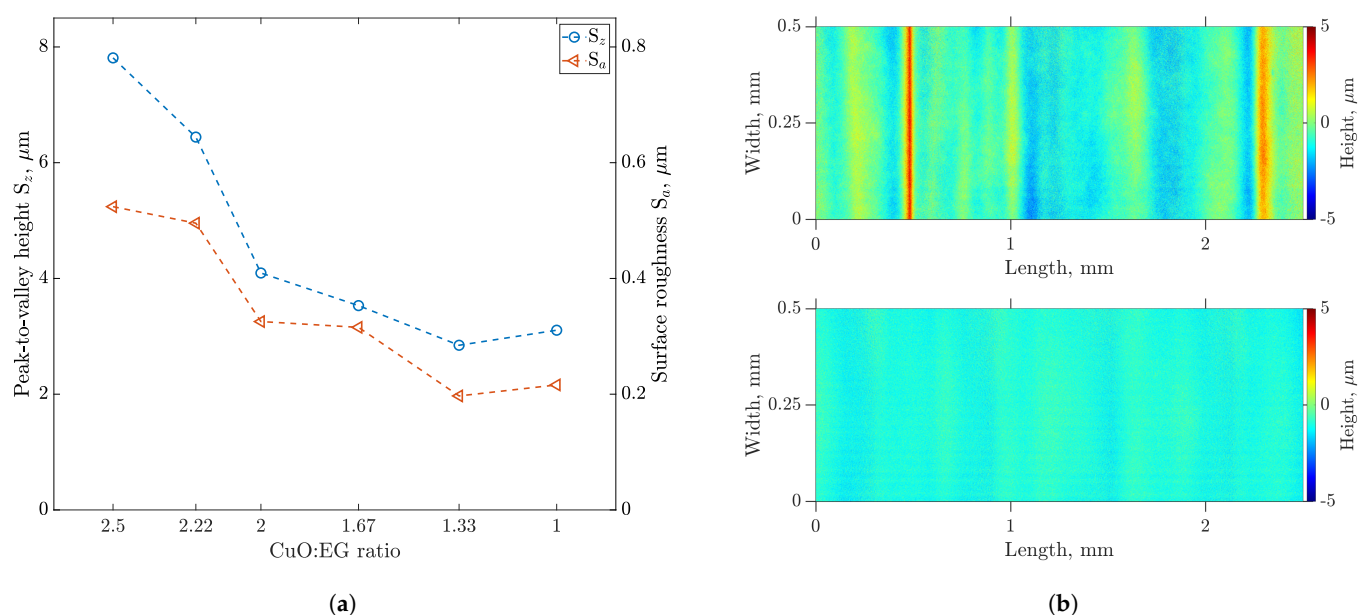


Figure 7. (a) Evolution of peak-to-valley height S_z and mean surface roughness S_a of the resulting prepared PC dry films with nanosuspension dilution as measured by LSM. (b) LSM images of coated PC with varying CuO:EG concentrations: top 2.5 (stock) and bottom 1.33. Please note the identical height scales for better comparability.

3.5. Generation of Copper Patterns

To demonstrate the influence of PC dilution grades on the RLS process and the resulting Cu structures, PC dry films with CuO:EG concentrations of 2.5 and 1.33 were processed using an amplified near-infrared femtosecond laser combined with a galvanometric scanner system. For this purpose, two-dimensional copper surfaces were generated by hatching according to the procedure described in [6,7]. The resulting electrodes are shown in Figure 8a, where the hatch direction was aligned in the direction of the grooves in the dry layers, and Figure 8b perpendicular. The inhomogeneities present in the PC layer from Figure 7 are reflected in the Cu structures. Figure 8c visualizes the application of the same laser parameters to homogeneous PC layers. This provides a significantly more homogeneous

appearance in terms of layer thickness distribution. The use of such an inhomogeneous copper layer, as produced with insufficient dilution, cannot produce reproducible electronic component requirements.

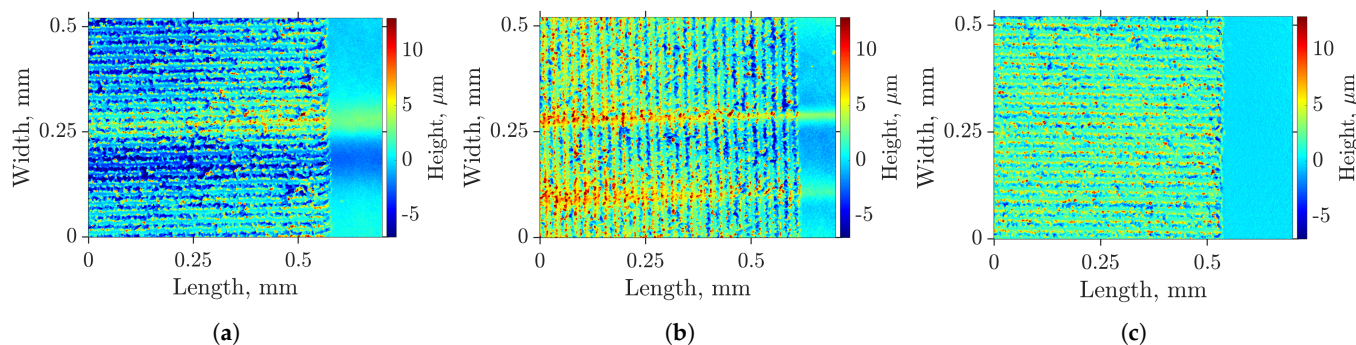


Figure 8. LSM images of copper electrodes from RLS processed precursors with varying CuO:EG concentrations: (a,b) 2.5 (stock) and (c) 1.33.

4. Discussion

The flow curves clearly indicate the shear thinning behavior of CuO nanosuspensions for the different dilution levels as described in the literature [25,26], classifying it as a non-Newtonian fluid. In their rheological start-up behavior at low shear rates, highly filled disperse systems usually show an apparently greater initial drop in viscosity. Here, the increase is due to the particle interaction of the highly filled system. The plate-shaped particles shown in the particle analyses are initially randomly oriented at low shear rates and become parallelized with increasing shear, leading to an associated decrease in viscosity [27]. Mueller et al. observed that this effect increases with increasing aspect ratio of the NPs [28]. In a majority of previous studies, spin coating was chosen as the coating method [8,15–19]. However, due to the shear thinning behavior of the PC, the coating thickness decreases outward from the center of rotation, making it difficult to achieve uniform coating thickness. Unlike spin coating, doctor blade coating is characterized by a constant shear stress on the PC during the process, resulting in uniform PC layers. In addition, the process is easily scalable to larger samples and requires less ink.

Hysteresis can be observed in the flow curves for all particle concentrations. When measuring the high concentrated nanosuspension (CuO:EG = 2.22), it is noticeable that the viscosity decreases after the initial shearing. For the higher dilutions, this effect occurs only at lower shear rates. It is assumed that in a highly filled nanofluid, particle conglomerates form without shear and are separated by shear. The smaller the particles in a nanofluid, the larger their specific surface area. The consequences of this separation by shear are stronger electrostatic forces, so that the viscosity also increases with smaller particles [29]. The result is an additional relaxation behavior after an initial increase in viscosity immediately after shearing. The simultaneous alignment of the plate-shaped particles outweighs this effect, so that the shear thinning behavior dominates. For this reason, viscosity decreases with increasing shear rate, as reflected by the flow curves and the 3ITT step two. However, when the shear rate is abruptly reduced, as in step three of the 3ITT, the dispersion-induced viscosity increase becomes dominant and the viscosity increases after shear. The more concentrated the suspension, the more particles are in contact and the more coagulates are present at the onset of shear, resulting in a greater viscosity difference. The exponential decrease in viscosity with increasing dilution was also observed by Kulkarni et al. in studies of CuO NPs in water with particle contents of up to 49.9 wt% [23]. At low particle concentrations, this dependence could also be demonstrated for the base solution EG. The process is similar to current approaches in battery and fuel cell technology for the production of anodes and cathodes. It therefore provides an approach for the production of continuous strands that could be subjected to multiple coating processes after drying.

Doctor blade coatings reflect the 3ITT results. At high CuO:EG ratios, there is a sharp jump in viscosity, which is reflected in the presence of grooves and the associated high S_a and S_z . Only when sufficiently diluted to a ratio of 1.33 or less, the PC has a high flowability immediately after shearing, so that the grooves formed during coating are smoothed out. Previous work [22] has shown, in connection with the presence of large agglomerates in the PC, that a homogeneous surface is urgently required in order to produce reproducible, homogeneous and defect-free Cu structures. Shestakov et al. also showed in the context of RLS with deep eutectic solvents that the layer thickness of the PC has a significant influence on the laser-generated Cu structure [30]. Accordingly, it is essential to adapt the viscoelastic behavior of the CuO-based RLS PC to the coating in order to minimize the presence of disturbances in the resulting layers. Since the EG volatilizes almost completely from the nanosuspension upon drying on the hotplate (in contrast to RLS studies where the PC is lasered in the liquid state [31,32]) and PVP is evaluated as a reducing agent [20], it is assumed that the thermochemical RLS process is not affected by an increased solvent content. It should be noted that in the context of the RLS process, it is not useful to vary the PVP content to adjust the rheological properties, although it has been shown that this can have an impact [33]. The amount of reducing agent PVP is critical for the chemical reduction process and copper formation [20]. Deviating from the most commonly used CuO:PVP ratio of 4.62 (resulting in CuO:PVP:EG = 60:13:27 [7,8,15]) to improve coating performance would therefore be counterproductive.

Arakane et al. [15] observed that at a CuO:EG ratio of 1.28 (50 wt% CuO) no homogeneous PC layers can be formed by spin coating. An ideal particle content of 60 wt% is concluded due to the increasing formation of surface deformations by agglomerate formation with decreasing particle content. The results shown in this work deviate from previous observations and show that a homogeneous surface can only be formed when the particle content is reduced to about 50 wt%. In addition to the different coating technique, we presume that this is primarily due to the milling process, which is associated with highly dispersed PC [22]. The degassing of the PC also prevents the formation of fine air bubbles during the drying process of the PC layer. Our previous studies have shown that RLS with PC diluted dropwise with EG produces high quality copper layers with surface conductivities of $0.278 \Omega/\text{sq}$ [22]. The present work now quantifies the exact dilution and helps to further optimize the laser-based process aspect in the future.

The selection of the materials COC as a representative of the polymer group and soda-lime glass already shows that different material classes can be coated with the adapted PC. Like the materials used here, most polymers must be plasma activated due to their low surface energy. It is assumed that with the help of this pre-treatment or the use of adhesion agents, a large number of other substrates can be metallized with the diluted PC.

5. Conclusions

In summary, this work demonstrates and discusses the influence of copper(II) oxide nanoparticle concentration on the rheological properties of precursors for reductive laser sintering, the coating quality during doctor blade coating and resulting copper electrodes. A highly filled, finely dispersed nanosuspension was first characterized with respect to particle size distribution and shape, and then diluted in several steps by adding the solvent ethylene glycol, so that particle:solvent (CuO:EG) ratios from 2.5 to 1.0 were investigated. Flow curves were obtained for each of these dilution steps. All suspensions exhibited strong shear thinning behavior, which explains the preference for the doctor blade method over spin coating. The viscosity of the PC decreases exponentially with decreasing particle concentration. In addition, three-interval thixotropy tests were performed to simulate the shear during doctor blade coating. In the 3ITT, the nanofluid exhibits an immediate increase in viscosity after strong shear, followed by relaxation behavior at constant shear. This effect is attenuated by dilution and is also reflected in the resulting dry layers after coating. While high particle concentrations in the range of 62 wt% lead to grooves and a peak-to-valley height of up to $7.8 \mu\text{m}$, which hinder the formation of homogeneous copper

layers during reductive laser sintering, this behavior can be avoided and reduced by 80% by choosing a lower particle concentration of 50.25%. The results of this work thus pave the way for reproducible metallization of a wide range of substrates.

Author Contributions: Conceptualization, K.B., D.M. and A.S.; methodology, K.B., D.M. and A.S.; validation, K.B. and D.M.; formal analysis, K.B. and D.M.; investigation, K.B. and D.M.; resources, A.S. and R.H.; writing—original draft preparation, K.B., D.M., A.S. and R.H.; writing—review and editing, K.B., D.M., C.E. and R.H.; visualization, K.B. and D.M.; supervision, R.H.; project administration, R.H.; funding acquisition, R.H. All authors have read and agreed to the published version of the manuscript.

Funding: This research was funded by German Federal Ministry of Education and Research (project EFP-LOC) grant number FKZ 13FH153KX0.

Data Availability Statement: Data are contained within the article.

Conflicts of Interest: The authors declare no conflicts of interest.

Abbreviations

The following abbreviations are used in this manuscript:

3ITT	Three-interval thixotropy test
COC	Cyclic olefin copolymers
Cu	Copper
CuO	Copper(II) oxide
EG	Ethylene glycol
LSM	Laser scanning microscopy
NPs	Nanoparticles
PC	Precursor
RLS	Reductive laser sintering
SEM	Scanning electron microscopy

References

1. Martins, P.; Pereira, N.; Lima, A.C.; Garcia, A.; Mendes-Filipe, C.; Policia, R.; Correia, V.; Lanceros-Mendez, S. Advances in Printing and Electronics: From Engagement to Commitment. *Adv. Funct. Mater.* **2023**, *33*, 2213744. [[CrossRef](#)]
2. Chandrasekaran, S.; Jayakumar, A.; Velu, R. A Comprehensive Review on Printed Electronics: A Technology Drift towards a Sustainable Future. *Nanomaterials* **2022**, *12*, 4251. [[CrossRef](#)] [[PubMed](#)]
3. Kamyshny, A.; Magdassi, S. Conductive nanomaterials for printed electronics. *Small* **2014**, *10*, 3515–3535. [[CrossRef](#)] [[PubMed](#)]
4. Li, W.; Sun, Q.; Li, L.; Jiu, J.; Liu, X.Y.; Kanehara, M.; Minari, T.; Sugauma, K. The rise of conductive copper inks: Challenges and perspectives. *Appl. Mater. Today* **2020**, *18*, 100451. [[CrossRef](#)]
5. Nam, V.B.; Giang, T.T.; Koo, S.; Rho, J.; Lee, D. Laser digital patterning of conductive electrodes using metal oxide nanomaterials. *Nano Converg.* **2020**, *7*, 23. [[CrossRef](#)] [[PubMed](#)]
6. Kefer, S.; Bischoff, K.; Roth, G.L.; Haubner, J.; Schmauss, B.; Hellmann, R. Tunable Bulk Polymer Planar Bragg Gratings Electrified via Femtosecond Laser Reductive Sintering of CuO Nanoparticles. *Adv. Opt. Mater.* **2021**, *9*, 2002203. [[CrossRef](#)]
7. Roth, G.L.; Haubner, J.; Kefer, S.; Esen, C.; Hellmann, R. Fs-laser based hybrid micromachining for polymer micro-opto electrical systems. *Opt. Lasers Eng.* **2021**, *137*, 106362. [[CrossRef](#)]
8. Kang, B.; Han, S.; Kim, J.; Ko, S.; Yang, M. One-Step Fabrication of Copper Electrode by Laser-Induced Direct Local Reduction and Agglomeration of Copper Oxide Nanoparticle. *J. Phys. Chem. C* **2011**, *115*, 23664–23670. [[CrossRef](#)]
9. Manshina, A.A.; Povolotskiy, A.V.; Ivanova, T.Y.; Tver'yanovich, Y.S.; Tunik, S.P.; Kim, D.; Kim, M.; Kwon, S.C. Effect of salt precursor on laser-assisted copper deposition. *Appl. Phys. A* **2007**, *89*, 755–759. [[CrossRef](#)]
10. Song, S.M.; Cho, S.M. Copper Ion Inks Capable of Screen Printing and Intense Pulsed-Light Sintering on PET Substrates. *ACS Appl. Electron. Mater.* **2022**, *4*, 1882–1890. [[CrossRef](#)]
11. Jones, J.; Snowdon, M.R.; Rathod, S.; Peng, P. Direct laser writing of copper and copper oxide structures on plastic substrates for memristor devices. *Flex. Print. Electron.* **2023**, *8*, 015008. [[CrossRef](#)]
12. Mizoshiri, M.; Aoyama, K.; Uetsuki, A.; Ohishi, T. Direct Writing of Copper Micropatterns Using Near-Infrared Femtosecond Laser-Pulse-Induced Reduction of Glyoxylic Acid Copper Complex. *Micromachines* **2019**, *10*, 401. [[CrossRef](#)] [[PubMed](#)]
13. Avilova, E.A.; Khairullina, E.M.; Shishov, A.Y.; Eltyshva, E.A.; Mikhailovskii, V.; Sinev, D.A.; Tumkin, I.I. Direct Laser Writing of Copper Micropatterns from Deep Eutectic Solvents Using Pulsed near-IR Radiation. *Nanomaterials* **2022**, *12*, 1127. [[CrossRef](#)] [[PubMed](#)]

14. Khairullina, E.; Shishov, A.; Gordeychuk, D.; Logunov, L.; Levshakova, A.; Sosnovsky, V.B.; Koroleva, A.; Mikhailovsky, V.; Gurevich, E.L.; Chernyshov, I.; et al. Rapid and effective method of laser metallization of dielectric materials using deep eutectic solvents with copper acetate. *J. Mater. Sci.* **2023**, *58*, 9322–9336. [[CrossRef](#)]
15. Arakane, S.; Mizoshiri, M.; Hata, S. Direct patterning of Cu microstructures using femtosecond laser-induced CuO nanoparticle reduction. *Jpn. J. Appl. Phys.* **2015**, *54*, 06FP07. [[CrossRef](#)]
16. Mizoshiri, M.; Ito, Y.; Arakane, S.; Sakurai, J.; Hata, S. Direct fabrication of Cu/Cu₂O composite micro-temperature sensor using femtosecond laser reduction patterning. *Jpn. J. Appl. Phys.* **2016**, *55*, 06GP05. [[CrossRef](#)]
17. Tumkin, I.I.; Khairullina, E.M.; Panov, M.S.; Yoshidomi, K.; Mizoshiri, M. Copper and Nickel Microsensors Produced by Selective Laser Reductive Sintering for Non-Enzymatic Glucose Detection. *Materials* **2021**, *14*, 2493. [[CrossRef](#)]
18. Huang, Y.; Xie, X.; Li, M.; Xu, M.; Long, J. Copper circuits fabricated on flexible polymer substrates by a high repetition rate femtosecond laser-induced selective local reduction of copper oxide nanoparticles. *Opt. Express* **2021**, *29*, 4453. [[CrossRef](#)]
19. Zhao, J.; Yu, Z.; Tu, Z.; Bian, H. Influence of Electrode Structure on Performance of Laser Direct Writing Cu-PI Flexible Humidity Sensor. *Micromachines* **2022**, *13*, 992. [[CrossRef](#)]
20. Binh Nam, V.; Thi Giang, T.; Lee, D. Laser digital patterning of finely-structured flexible copper electrodes using copper oxide nanoparticle ink produced by a scalable synthesis method. *Appl. Surf. Sci.* **2021**, *570*, 151179. [[CrossRef](#)]
21. Back, S.; Kang, B. Low-cost optical fabrication of flexible copper electrode via laser-induced reductive sintering and adhesive transfer. *Opt. Lasers Eng.* **2018**, *101*, 78–84. [[CrossRef](#)]
22. Bischoff, K.; Esen, C.; Hellmann, R. Preparation of Dispersed Copper(II) Oxide Nanosuspensions as Precursor for Femtosecond Reductive Laser Sintering by High-Energy Ball Milling. *Nanomaterials* **2023**, *13*, 2693. [[CrossRef](#)]
23. Kulkarni, D.P.; Das, D.K.; Chukwu, G.A. Temperature dependent rheological property of copper oxide nanoparticles suspension (nanofluid). *J. Nanosci. Nanotechnol.* **2006**, *6*, 1150–1154. [[CrossRef](#)] [[PubMed](#)]
24. Dzido, G.; Chmiel-Kurowska, K.; Gierczycki, A.; Jarzębski, A.B. Application of Klein's equation for description of viscosity of nanofluid. In *19th European Symposium on Computer Aided Process Engineering; Computer-Aided Chemical Engineering 1570-7946*; Jeżowski, J., Ed.; Elsevier: Amsterdam, The Netherlands; London, UK, 2009; Volume 26, pp. 955–960. [[CrossRef](#)]
25. Patra, A.K.; Nayak, M.K.; Misra, A. Viscosity of nanofluids—A Review. *Int. J. Thermofluid Sci. Technol.* **2020**, *7*, 070202. [[CrossRef](#)]
26. Ye, X.; Kandlikar, S.G.; Li, C. Viscosity of nanofluids containing anisotropic particles: A critical review and a comprehensive model. *Eur. Phys. J. E Soft Matter* **2019**, *42*, 159. [[CrossRef](#)] [[PubMed](#)]
27. Kuhn, W.; Kuhn, H. Die Abhängigkeit der Viskosität vom Strömungsgefälle bei hochverdünnten Suspensionen und Lösungen. *Helv. Chim. Acta* **1945**, *28*, 97–127. [[CrossRef](#)]
28. Mueller, S.; Llewellyn, E.W.; Mader, H.M. The rheology of suspensions of solid particles. *Proc. R. Soc. A Math. Phys. Eng. Sci.* **2010**, *466*, 1201–1228. [[CrossRef](#)]
29. Chang, H.; Jwo, C.S.; Lo, C.H.; Tsung, T.T.; Kao, M.J.; Lin, H.M. Rheology of CuO nanoparticle suspension prepared by asns. *Rev. Adv. Mater. Sci.* **2005**, *10*, 128–132.
30. Shestakov, D.; Khairullina, E.; Shishov, A.; Khubezhov, S.; Makarov, S.; Tumkin, I.; Logunov, L. Picosecond laser writing of highly conductive copper micro-contacts from deep eutectic solvents. *Opt. Laser Technol.* **2023**, *167*, 109777. [[CrossRef](#)]
31. Zhou, X.; Guo, W.; Zhu, Y.; Peng, P. The laser writing of highly conductive and anti-oxidative copper structures in liquid. *Nanoscale* **2020**, *12*, 563–571. [[CrossRef](#)]
32. Li, Y.; Zhou, X.; Chen, J.; Guo, W.; He, S.; Gao, S.; Peng, P. Laser—Patterned Copper Electrodes for Proximity and Tactile Sensors. *Adv. Mater. Interfaces* **2020**, *7*, 1901845. [[CrossRef](#)]
33. Sato, T.; Kohnosu, S. Effect of polyvinylpyrrolidone on the physical properties of titanium dioxide suspensions. *Colloids Surf. A Physicochem. Eng. Asp.* **1994**, *88*, 197–205. [[CrossRef](#)]

Disclaimer/Publisher's Note: The statements, opinions and data contained in all publications are solely those of the individual author(s) and contributor(s) and not of MDPI and/or the editor(s). MDPI and/or the editor(s) disclaim responsibility for any injury to people or property resulting from any ideas, methods, instructions or products referred to in the content.